



## **Effect of fluid damping on vibration response of immersed rotors**

**Mahmud Rasheed Ismail<sup>1</sup>, Mustafa Asaad Hussein<sup>2</sup>**

<sup>1</sup> Prosthetics and Orthotics Engineering Department, AL-Nahrain University, Ministry of Higher Education & Scientific Research, Iraq.

<sup>2</sup> Mechanical Engineering Department, AL-Nahrain University, Ministry of Higher Education & Scientific Research, Iraq.

### **Abstract**

As immersed rotors vibrate in a viscous media such as fluid, a considerable amount of damping may be generated due to the interaction phenomena between the rotor components and the fluid media. Such damping is depending on many factors such as; fluid drag, fluid friction, turbulence, vortex and so on. Immersed rotors find their application in many engineering fields such as Marines machines, gear box, turbine and pumps. In the present work, a mathematical model is attempted to investigate the dynamical behavior immersed rotor. The model takes into account the effects of the most rotordynamic parameters, namely; fluid drag, damping and stiffness of bearing, unbalance and gyroscopic effects of the attached disc, and elastic bending and internal damping of rotor shaft. Four types of fluid are employed as a fluid immersing media which are; Air, Water, SAE 20 and SAE 40 oils. The experimental apparatus includes a sample rotor with single disc and plastic fluid container. Two proximate sensors are employed for measuring the unbalance response and orbits shapes under different rotor speeds, and discs size and locations. Modal analysis is employed for solving the governing equation of vibration motion. To check the validity of the mathematical model the theoretical results are compared with the experimental results. It is found that; the theoretical results are in a good agreement with the experimental ones, where the maximum error is not exceeded (6.8 %), and that; the fluid damping can highly reduce the peak amplitude of the unbalance response (up to 60 %) however, it has slight effect on the critical speeds which are highly affected by the size and location of the attached disc.

**Copyright © 2016 International Energy and Environment Foundation - All rights reserved.**

**Keywords:** Rotordynamics; Immersed rotor; Campbell diagram; Orbits; Unbalance response.

### **1. Introduction**

In many applications such as gearbox, submerge machines, pumps, turbines and marines machines, rotors interacts with the surrounding fluid which may be water, oil or gas. The theoretical analysis and modeling of this type of Immersed rotors is so complicated, however under successive assumptions a reasonable models can be served.

In 1869, the first attempt to formulate the dynamics of rotor had been put forward by Rankin. However the first acceptable simplified model for rigid rotors had been proposed by Jeffcott in 1919. Proposed simple analysis of rotor model by using SDOF vibration analysis. It found that their existed a speed at which high vibration can occurs [1]. From that time till now enormous theoretical and experimental

works has been achieved. A comprehensive survey about this object can be found in many references such as Rao [2] and Adems [3].

There are many kinds of dynamical force and moments contribute the dynamical behavior of rotors. First the elasticity and damping forces of oil film at bearings. Second; the gyroscopic and inertial (lateral and rotational) effect of the attached disc as it spins. Third; the external forces dynamical unbalancing forces. Including of these effects, will complicate the analysis even for the simplest models [4]. However, for immersed types of rotor or for rotors interact with fluid media another set of parameters must be taken into account. This make the analysis becomes more tedious, since the dynamic and vibration of fluid-structure interaction by itself [5]. The main parameters dealing with the immersed rotor are; fluid damping mechanism, vortex, turbulent, fluid shear and drag, the added mass and stiffness and so on [6]. The analysis of rotor was normally achieved via numerical methods such as Finite Element [7], Lumped analysis and Transfer Matrix method [8]. The accurate analysis demand four degree of freedom for the individual station (two translations and two rotations). A large number of stations are needed (more than 300) for accurate numerical analysis [5]. This is leading to a huge global matrix for analyzing the Eigen value problem and frequency response. Analytical methods are seldom used except for simple or high approximated models [9].

In the present work, the dynamical behavior of immersed rotor is analyzed by developing a mathematical model takes into account the main rotor parameters as well as the interaction parameters assuming linear behavior for the interacted fluid. The problem is solved analytically by employing Modal analysis approach. An appropriate shape functions as basis functions necessary for performing the analysis was selected [10]. Such functions take into account the elastic deformation of the shaft as well as the possibility of rigid body translation and rotation.

**2. Mathematical model**

In driving the mathematical models it is assumed that the shaft obeys Rayleigh beam theory where the shear deformation is neglected. The disc is rigid, however the effect of transitory and rotary inertia and gyroscopic are included. The journal bearings are assumed to be Isotropic and exhibit a linear stiffness and damping. The viscosity of the surrounding fluid is constant throughout the oil film. The fluid flow is laminar, so that Reynolds equation can be applied. The shear force due to fluid-rotor interaction is assumed to be linear. Figure 1a shows the schematic drawing of the immersed rotors model. It contains an elastic shaft supported by two journals bearing and holding a disc. The disc is allowed to rotate in a fluid media.

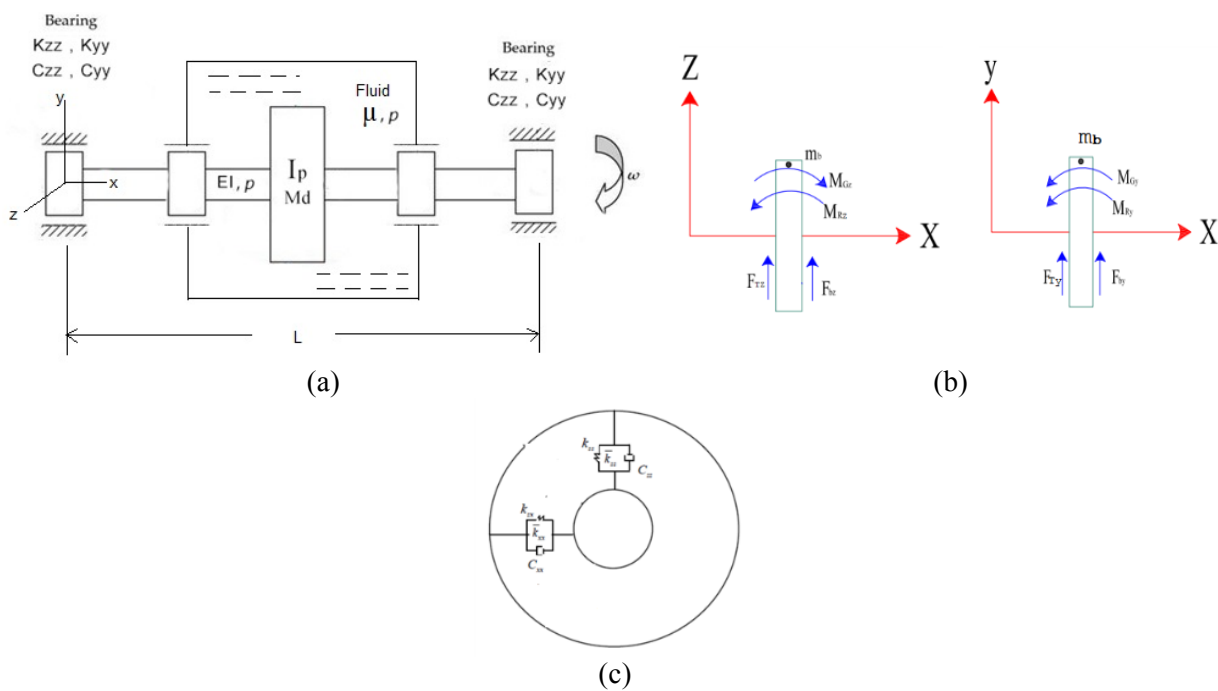


Figure 1. (a) Rotor system, (b) Loads on disc, (c) Bearing stiffness and damping.

The governing equation of motion at the two orthogonal planes x-y and x-z along the shaft natural axes can be written as [11];

$$EI \frac{\partial^4 w}{\partial x^4} + \rho A \frac{\partial^2 w}{\partial t^2} + C \frac{\partial w}{\partial t} - \rho I \frac{\partial^2}{\partial x^2} \left( \frac{\partial^2 w}{\partial t^2} \right) - 2\rho I \omega_{sp} \frac{\partial^2}{\partial x^2} \left( \frac{\partial v}{\partial t} \right) = f_z(x, t) \quad (1)$$

$$EI \frac{\partial^4 v}{\partial x^4} + \rho A \frac{\partial^2 v}{\partial t^2} + C \frac{\partial v}{\partial t} - \rho I \frac{\partial^2}{\partial x^2} \left( \frac{\partial^2 v}{\partial t^2} \right) + 2\rho I \omega_{sp} \frac{\partial^2}{\partial x^2} \left( \frac{\partial w}{\partial t} \right) = f_y(x, t) \quad (2)$$

Where  $w$  and  $v$  are the displacements along  $z$  and  $y$  axes respectively.

The R.H.S terms of Eqs. (1) and (2) represent the dynamical forces due to the bearing and discs at x-z and x-y planes.

In case of,  $f_z(x, t)$  these are as follows;

1- Bearing spring forces Figure 1c;

$$F_{SZ} = -K_{iz} w(x, t) \quad (3)$$

2- Bearing damping forces;

$$F_{DZ} = -C_{iz} \frac{\partial w}{\partial t} \quad (4)$$

3- Disc translation inertial forces Figure 1b:

$$F_{TZ} = -m_j \frac{\partial^2 w}{\partial t^2} \quad (5)$$

4- Disc imbalances forces;

$$F_{bz} = \frac{\alpha}{L} m b_j e \omega_{sp}^2 \sin \omega_{sp} t \quad (6)$$

5- Disk gyroscopic moments;

$$M_{GZ} = -J_j \omega_{sp} \frac{\partial}{\partial t} \left( \frac{\partial v}{\partial x} \right) \quad (7)$$

6- Disc rotational inertia moments;

$$M_{RZ} = -J_j \frac{\partial^2}{\partial t^2} \left( \frac{\partial w}{\partial x} \right) \quad (8)$$

7- Drag force due to fluid interaction

According to the assumptions stated above and referring to Figure 2, one can write;

$$\tau = \mu \frac{du}{dx} \quad (9)$$

Due to vibration the center velocity of the disc is  $dz/dt$  and the surface velocity at a ring element with radius  $r$  is  $\Omega r$  while the velocity at wall of the container is zero, so that Eq. (9) becomes;

$$\tau = \mu \frac{(\Omega r + \dot{z}) - 0}{s} \quad (10)$$

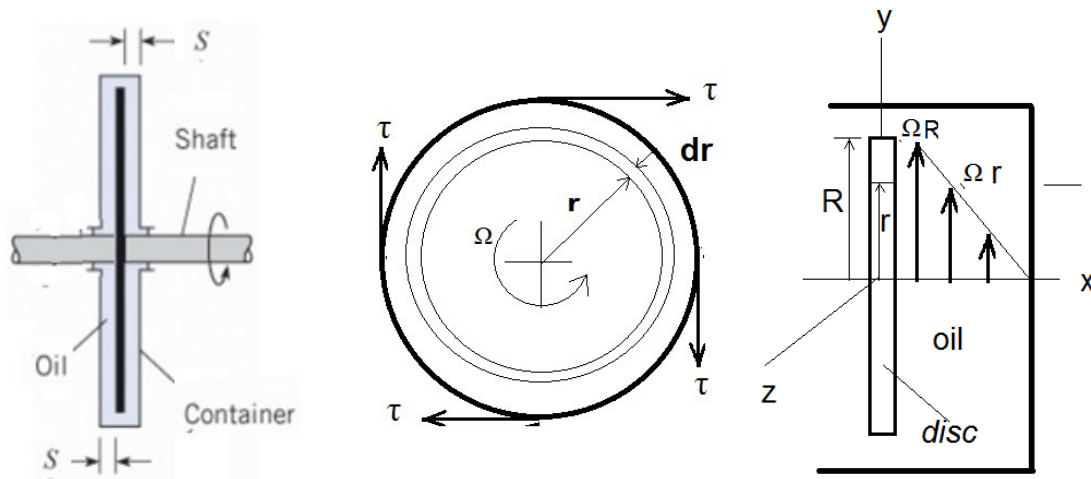


Figure 2. Fluid shear and drag forces on disc.

The shear force is;

$$dF_z = \tau A \quad (11)$$

Where A is the area of the ring element of the disc and equal  $2\pi r dr$ . The total shear exerted on one face of the disc is;

$$F_z = 2\pi \int_0^R \mu (\Omega + z/r) \frac{r^2}{S} = \frac{2\pi\mu\Omega R^3}{3S} + \frac{\pi\mu z}{S} \quad (12)$$

Finally, the total force on the two side of the disc is;

$$F_z = \frac{4\pi\mu\Omega R^3}{3S} + \frac{2\pi\mu z}{S} \quad (13)$$

In case of  $f_y(x, t)$  the same procedures are repeated, but with successive replacement of w by v.

To introduce Modal analysis, a solution in term of the beam normal modes may be taken. Let such solutions of eqs (1) and (2) be [12];

$$\begin{aligned} w(x, t) &= \sum_{s=1}^N \phi_s(x) q_s(t) + \phi_T(x) q_T(t) + \phi_R(x) q_R(t) \\ v(x, t) &= \sum_{s=1}^N \psi_s(x) p_s(t) + \psi_T(x) p_T(t) + \psi_R(x) p_R(t) \end{aligned} \quad (14)$$

In eqs. (14);  $\phi_s(x)$  and  $\psi_s(x)$  stand for the normal modes of beam free vibration,  $\phi_T$  and  $\psi_T$  for translational modes and  $\phi_R$ ,  $\psi_R$  for rotational modes in z and y directions, respectively.

In the absence of all the forces and moments the normalized modes shapes  $\phi_s(x)$  and  $\psi_s(x)$  are those of free-free beam which take the following form, [13]:

$$\phi_s(x) = \psi_s(x) = \sin \lambda_s x + \sinh \lambda_s x - \sigma_s (\cos \lambda_s x + \cosh \lambda_s x) \quad (15)$$

Where;

$$\sigma_s = \frac{\sinh \lambda_s - \sin \lambda_s}{\cosh \lambda_s - \cos \lambda_s} \quad (16)$$

$\lambda_s$  is the Eigen values of the free-free beam.

The normalized modes of translational and rotational modes may be taken as;

$$\begin{aligned}\phi_T(x) &= \psi_T(x) = 1 \\ \phi_R(x) &= \psi_R(x) = x/l\end{aligned}\quad (17)$$

Substitute Eq. (14) to (17) into Eqs. (1) and (2), and following Modal analysis procedure in which another series for the r modes is chosen as:  $\phi_r(x) = \sum_{r=1}^N \phi_r(x) + 1 + x/l$

Now, multiply, integrate from 0 to L and make use of the orthogonality of the normal modes, the following matrix equation can be obtained as;

$$[K_z]\{q\} + [C_z]\{\dot{q}\} - [G]\{\dot{p}\} + [M]\{\ddot{q}\} = \{W\}\cos\Omega t + [N]\cos\Omega t \quad (18)$$

$$[K_y]\{p\} + [C_y]\{\dot{p}\} + [G]\{\dot{q}\} + [M]\{\ddot{p}\} = \{W\}\sin\Omega t + [N]\sin\Omega t \quad (19)$$

Where:  $[K_z] = [A] + K_{zz1}^*[H] + K_{zz5}^*[L] + K_{zz2}^*[H] + K_{zz4}^*[L]$

$[K_y] = [A] + K_{yy1}^*[H] + K_{yy5}^*[L] + K_{yy2}^*[H] + K_{yy4}^*[L]$

$[C_z] = C_{zz1}^*[H] + C_{zz5}^*[L]$

$[C_y] = C_{yy1}^*[H] + C_{yy5}^*[L]$

$[G] = I_p^*\Omega[V]$

$[M] = m_d^*[T] + I_T^*[V] + [B]$

$\{W\} = m_b^* \cdot e \cdot \Omega^2 \{\bar{W}\}$

$[N] = \zeta + \varepsilon [\bar{N}]$

And;

$$\begin{aligned}K_{iz}^* &= \frac{K_{iz}L^3}{EI}, \quad K_{iy}^* = \frac{K_{iy}L^3}{EI}, \quad C_{iy}^* = \frac{C_{iy}}{\sqrt{\rho AEI}}, \quad C_{iz}^* = \frac{C_{iz}}{\sqrt{\rho AEI}}, \quad m_{b_j}^* = \frac{mb_j}{\rho AL}, \quad m_j^* = \frac{m_j}{\rho AL}, \\ \bar{e} &= \frac{e}{L}, \quad \bar{a} = \frac{a}{L}, \quad \bar{b} = \frac{b}{L}, \quad \zeta = \frac{2\pi\mu\Omega R^3}{3S}, \quad \varepsilon = \frac{\pi\mu}{S}\end{aligned}\quad (20)$$

The Elements of matrix [A], [B], [L], [H], [T], [V], [W] and [N] are as the follows:

$$\begin{aligned}a_{s,r} &= \int_0^L \phi_s^{IV}(x)\phi_r(x)dx = \int_0^1 \varphi_s^{IV}(x)\varphi_r(x)dx, \quad a_{s,1+N} = \int_0^1 \phi_s^{IV}(x)dx = \int_0^1 \varphi_s^{IV}(x)dx \\ a_{s,2+N} &= \int_0^L x\phi_s^{IV}(x)dx = \int_0^1 x\varphi_s^{IV}(x)dx, \quad b_{s,r} = \int_0^L \phi_s(x)\phi_r(x)dx = \int_0^1 \varphi_s(x)\varphi_r(x)dx \\ b_{1+N,r} &= \int_0^L \phi_r(x)dx = \int_0^1 \varphi_r(x)dx, \quad b_{2+N,r} = \int_0^L x\phi_r(x)dx = \int_0^1 x\varphi_r(x)dx \\ b_{s,1+N} &= \int_0^L \phi_s(x)dx = \int_0^1 \varphi_s(x)dx, \quad b_{1+N,1+N} = \int_0^1 (1)dx = L, \quad b_{2+N,1+N} = b_{1+N,2+N} = \int_0^1 x \cdot dx = \frac{L^2}{2}, \\ b_{s,2+N} &= \int_0^L \phi_s(x) \cdot x \cdot dx = \int_0^1 \varphi_s(x) \cdot x \cdot dx \\ l_{s,2+N} &= \int_0^L \phi_s''(x)x dx = \int_0^1 \varphi_s''(x)x dx, \quad l_{s,r} = \int_0^L \phi_s''(x)\phi_r(x)dx = \int_0^1 \varphi_s''(x)\varphi_r(x)dx, \quad s_{s,1+N} = \int_0^L \phi_s''(x)dx \\ &= \int_0^L \psi_s''(x)dx\end{aligned}$$

$$\begin{aligned}
 h_{s,r} &= \int_0^L \phi_r(x)\phi_s(x)dx = \int_0^L \psi_r(x)\psi_s(x)dx, h_{1+N,r} = h_{s,1+N} = \int_0^L \phi_s(x)dx = \int_0^L \psi_s(x)dx, \\
 h_{1+N,1+N} &= 1 h_{2+N,r} = h_{2+N,1+N} = h_{2+N,r} = h_{2+N,1+N} = h_{2+N,2+N} = 0 \\
 t_{s,r} &= \int_0^1 \phi_r(x)\phi_s(x)dx = \int_0^1 \psi_r(x_2)\psi_s(x)dx, t_{1+N,r} = t_{s,1+N} = \phi_s(\zeta_2) = \psi_s(\zeta), t_{1+N,1+N} = 1 \\
 t_{2+N,r} &= t_{2+N,1+N} = t_{2+N,r} = t_{2+N,1+N} = t_{2+N,2+N} = 0 \\
 v_{s,r} &= \phi'_r(x_2)\phi'_s(x_2) = \psi'_r(x)\psi'_s(x), \\
 v_{s,1+N} &= v_{s,2+N} = v_{1+N,r} = v_{1+N,1+N} = v_{1+N,2+N} = v_{2+N,r} = v_{2+N,1+N} = v_{2+N,2+N} = 0 \\
 w_{1,s} &= \phi_r(x), w_{1,1}=1, w_{1,2}=x/L \\
 N_{s,r} &= \phi_r(x_3)\phi_s(x_3) = \varphi_r(x_3)\varphi_s(x_3), N_{1+N,r} = N_{s,N+1} = \phi_s(x_3) = \varphi_r(x_3), N_{2+N,r} = N_{2+N,1+N} = \\
 N_{2+N,r} &= N_{2+N,1+N} = N_{2+N,2+N} = 0 \tag{21}
 \end{aligned}$$

2.1 Unbalance response, critical speeds and orbit shapes

Eqs. (18) and (19) can be combined in a single equation by using the following complex vector[14];

$$\{u\} = \{q\} + i\{p\} \tag{22}$$

$$[K]\{u\} + [C]\{\dot{u}\} + i\Omega[G][I]\{\dot{u}\} + [M][I]\{\ddot{u}\} = (\{W\} + i\{N\})e^{i\Omega t} \tag{23}$$

The steady state response of eq.(23) can be written as;

$$\{u\} = \left[ [K] + i\Omega[C] + i\Omega[G][I] - \Omega^2[M][I] \right]^{-1} \{Z\}e^{i\Omega t} \tag{24}$$

Where  $\{Z\} = \{W\} + i\{N\}$

For specified rotor the complex generalized coordinate represented by the vector  $\{u\}$  can be found from which  $\{q\}$  and  $\{p\}$  are readily available in y and z directions, respectively. The displacement of the unbalance response then can be found at any rotor section from Eqs (14). If the displacement in of the two orthogonal axes is combined together the orbit response can be found and plotted.

3. Experimental investigation

The aim of the experimental work is to justify some of the theoretical results. For this purpose, a sample model of rotor consisted of mild steel elastic shaft supported on two identical journal bearings is constructed. Two different sizes of discs are prepared as a load; a plastic container box was designed for immersing the disc in fluid media. The container is made from transparent plastic to visualize the fluid and disc motion. The main specifications of the rotor components are given in Table1. A photograph for the test rig is shown in Figure 3.

The rotor is driven by an electrical motor with variable speed of (0-2500) RPM. To reduce the undesired effect of the motor vibration which may interfere with the rotor response, a PVC coupling is used. A special attention was made for aligning the shaft with the motor shaft and the bearings to insure center to center alignment which is necessary for reducing the misalignment effect on the response. Two proximate probes are employed to detect the relative displacement of the shaft journal and fixed at the bearing housing in two orthogonal axes as shown in Figure 4.

Table 1. Specifications of the rotor model.

Bearing(1)	Bearing (2)	Disc(1)	Disc(2)	Shaft
$K_{xx1}=17.249 \times 10^6 \text{ N/m}$	$K_{xx}=17.25 \times 10^6 \text{ N/m}$	$d_3=0.27 \text{ m}$	$d_2=0.166 \text{ m}$	$L_s=1 \text{ m}$
$K_{yy1}=1.294 \times 10^6 \text{ N/m}$	$K_{yy}=1.29 \times 10^6 \text{ N/m}$	$t_3=0.022 \text{ m}$	$t_2=0.02 \text{ m}$	$d_s=0.019 \text{ m}$
$C_{zz1}=3.08 \times 10^5 \text{ Ns/m}$	$C_{zz}=3.1 \times 10^5 \text{ Ns/m}$	$\rho_3=8205 \text{ kg/m}^3$	$\rho_2=8205 \text{ kg/m}^3$	$E=205 \times 10^9 \text{ N/m}^2$
$C_{yy1}=2.05 \times 10^4 \text{ Ns/m}$	$C_{yy}=2.1 \times 10^4 \text{ Ns/m}$	$m_b=0.22 \text{ kg}$	$m_b=0.22 \text{ m}$	$\rho_s=7800 \text{ kg/m}^3$
		$r=0.05 \text{ m}$	$r=0.05 \text{ m}$	damp ratio =0.01

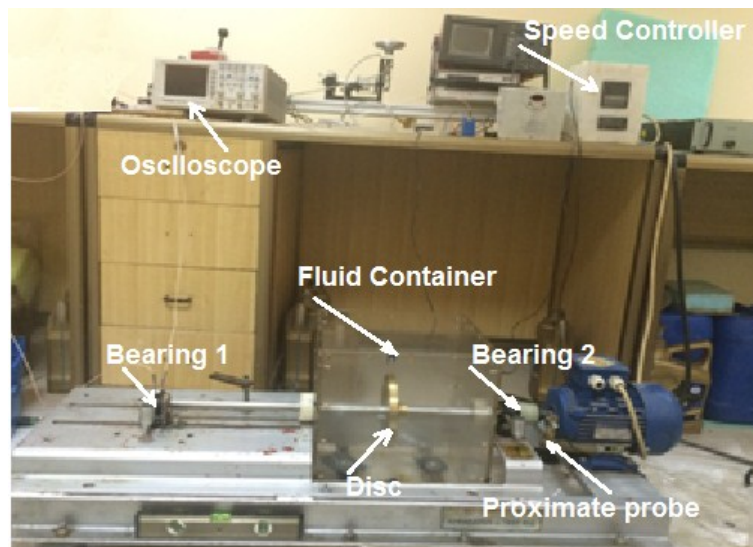


Figure 3. The test rig.

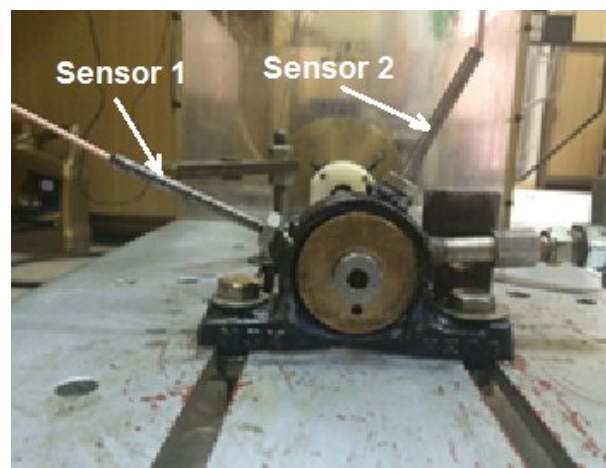


Figure 4. Locations of proximate sensors.

The block diagram of the connection layout of the sensors and controller are shown in Figure 5. The main task of the experimental work is to measure unbalance response, critical speeds and orbit shapes for four types of fluid which are; Air, Water and SAE 20 and SAE 40 oils, and investigate the effect of changing the size and position of the attached disc on the response.

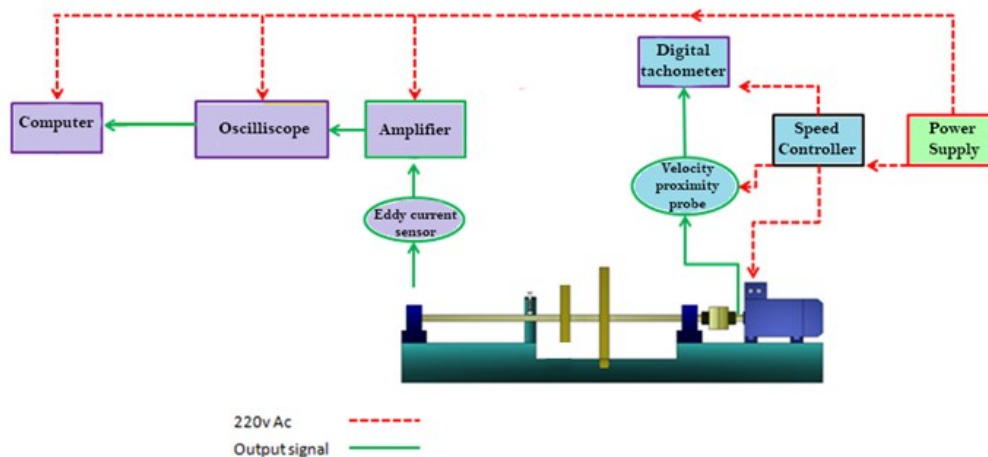


Figure 5. Connecting layout of sensors and controller.

In measuring the unbalance response one of the discs was attached to the shaft at two positions (mid and one third). The container was filled with fluid. The speed of the motor was increased gradually and the displacement from one proximate sensor is recorded and observed on the oscilloscope. The response curve was acquired to the computer and plotted. The critical speed then found from the peak response curve. Then the test was repeated for other types of fluids, and other disc size and disc location. The second sets of experiments were carried to evaluated orbit shape. In this case two sensors in appendicular positions are used. The outputs signal of the first sensor is connected channel A of the oscilloscope while the output of the second to channel B. Now by using the adding feature available in the oscilloscope the orbit shape can be plotted on the screen. Finally, the data were acquired to the computer were the result is saved and plotted.

#### 4. Results and discussions

The theoretical results of the unbalance response calculated from Eqs. (24) and (14) are plotted in Figure 6. MATLAB version Rb2012 is used for calculating and plotting. Four cases are investigate which are; case1: For large disc at mid span, case 2: For large disc at one -third span, case 3; Small disc at mid span and case 4: Small disc at one- third span. For any case four types of fluid are tested which are; air, water, oil SAE 20, oil SAE 40. Two important points can be clearly concluded form Figure 6, first; increasing of fluid viscosity will decrease the unbalance amplitude without affecting the critical speed (speed under peak response). The percentage reduction in amplitude relative to the air are presented in Table 2, second, the critical speed are clearly affected by changing the disc size and location. This behavior tells that; the effect of the surround fluid has a damping effect on the vibration of rotor and can reduce the stress and resonance.

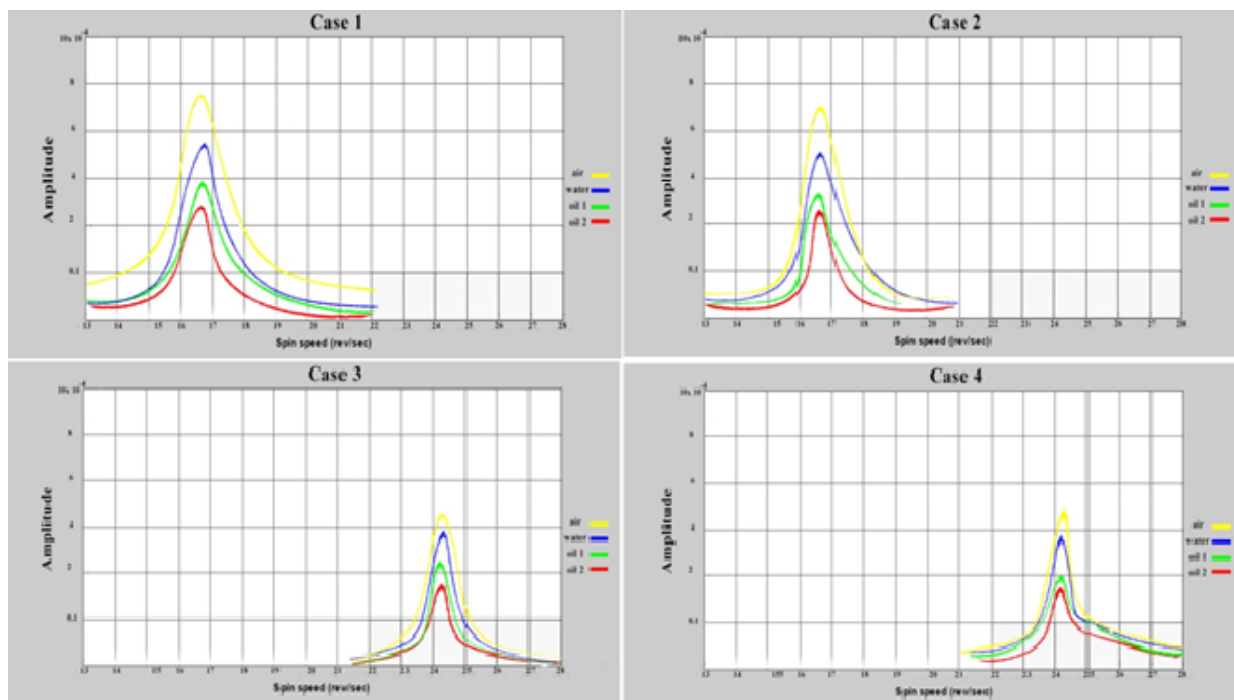


Figure 6. Theoretical unbalance response and critical speed of four disc cases (see text).

Table 2. Percentage reduction in rotor amplitude relative to the air.

case	Disc size and location	water	Oil SAE 20	Oil SAE 40
1	Large disc $x = L/3$	26.5 %	45.7%	57.8
2	Large disc $\zeta = L/2$	30 %	54%	60%
3	Small disc $\zeta = L/3$	18.7	39.7	48.5
4	Small disc $\zeta = L/2$	20.1	53.6	59.3

To justify the theoretical model and make a comparison of the results the same cases now investigated experimentally. The results of the experimental unbalance response curves are presented in Figure 7. Again the same behaviors are observed from these curves which relating the damping effect of the fluid and the critical speeds. To check the validity of the model the critical speeds are extracted from Figures 6 and 7 and collected in Table 3. The percentage error is calculated in the same table. As it can be seen from the table the good agreement between the theory and experiment where the maximum error in the critical speeds are not exceeded (6.8%).

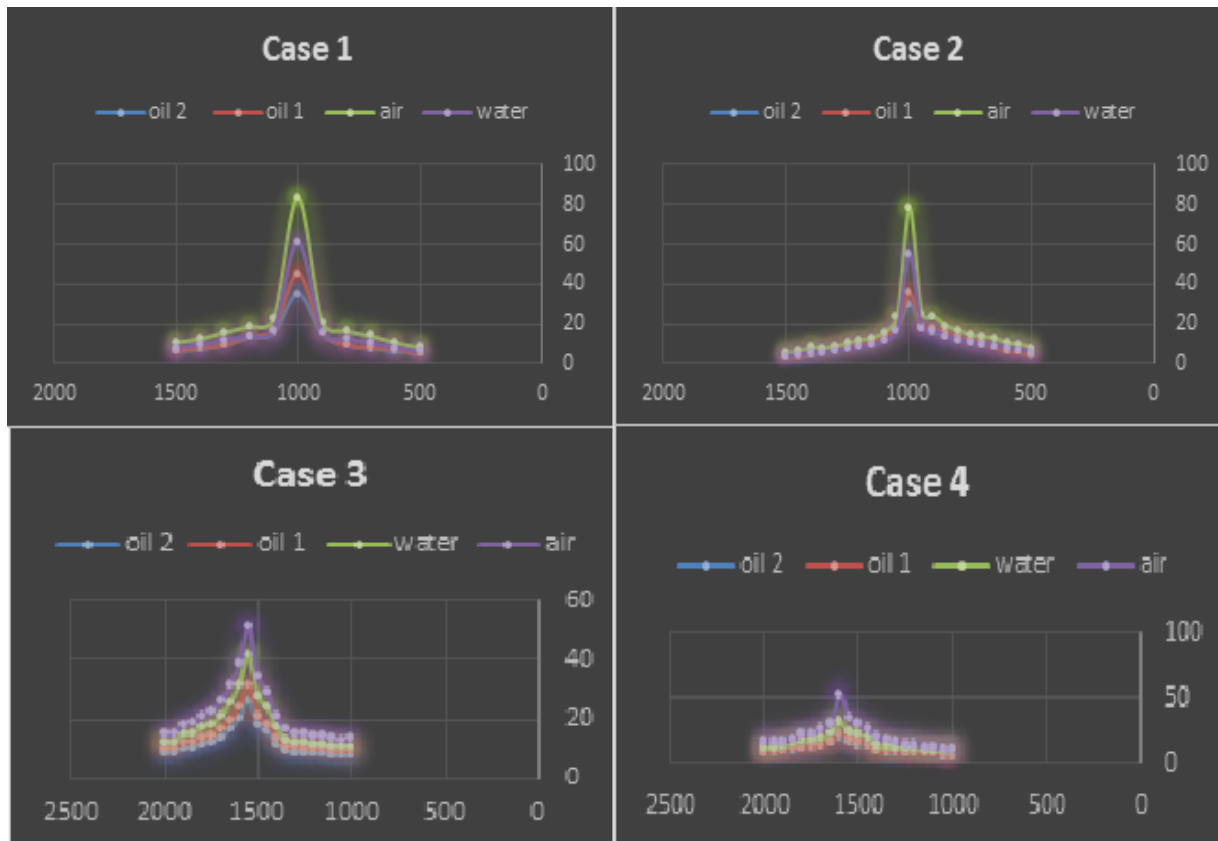


Figure 7. Experimental unbalance response for four cases (see text).

Table 3. Theoretical and experimental critical speeds.

Case	Disc size and location		Air	water	Oil SAE 20	Oil SAE 40	Max error %
1	large disc $x = L/3$	Theo.	936	1005	1002	945	-6.8
		Exp.	1000	1000	1000	1000	
2	large disc $x = L/2$	Theo.	940	1007	1004	951	-6.38
		Exp.	1000	1000	1000	1000	
3	small disc $x = L/3$	Theo.	1464	1472	1460	1470	-4.2
		Exp.	1575	1575	1575	1575	
4	Small disc $x = L/2$	Theo.	1458	1446	1449	1445	-3.7
		Exp.	1585	1585	1585	1585	

In Figures 8 and 9 plots of orbit shapes of shaft journal are presented. In Figure 8 the orbits are for the four cases of discs stated above with considering the air as a surrounding fluid while Figure 9 is for using SAE 40 oil as surrounding fluid. For the comparison purpose the theoretical orbits are also plotted in the same figures. A successful inspection of the two figures indicates the irregularity in the shapes in case of using the high viscous fluid. This can be attributed to the fact that; the orbit shapes are highly related with the damping and the existence of non-linearity in vibration motion due to the interaction between the rotor and the adjacent fluid. Since the present mathematical model based on linear assumption it is difficult to detect the irregularity in the shape, however the contour is in reasonable accuracy.

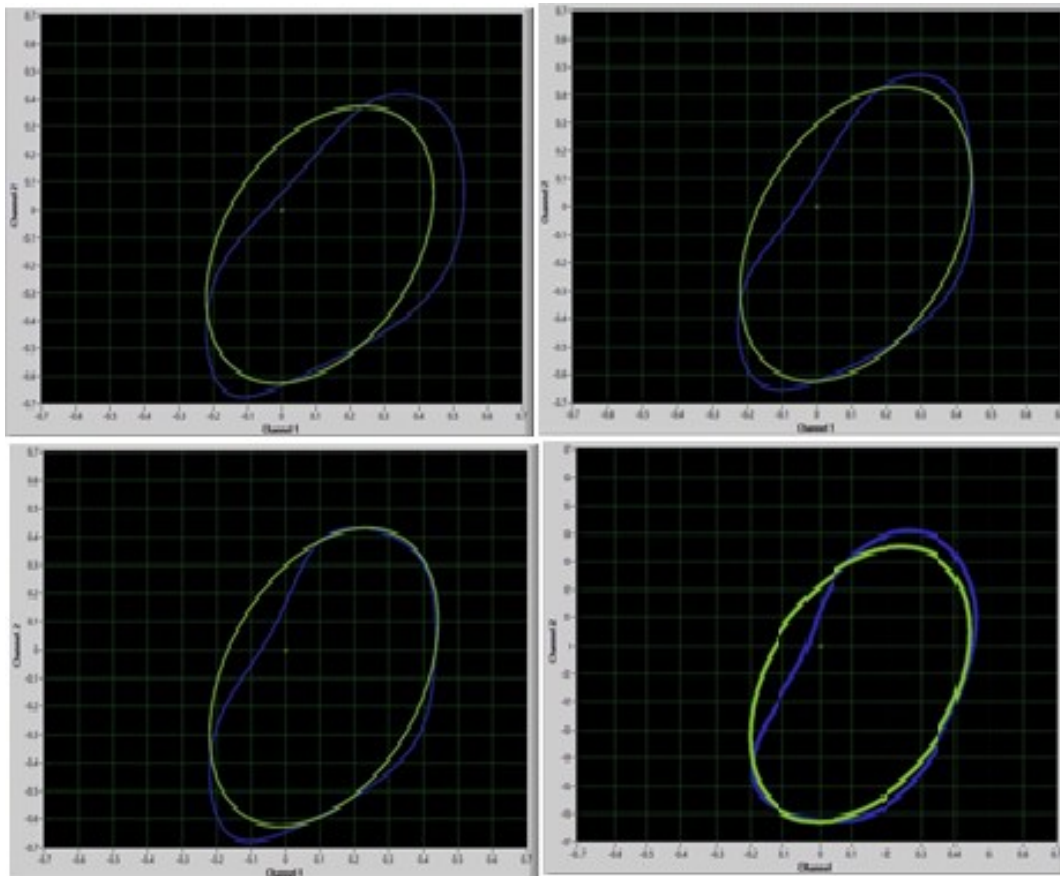


Figure 8. Orbit shapes for shaft journal rotates in water for four cases (see text).

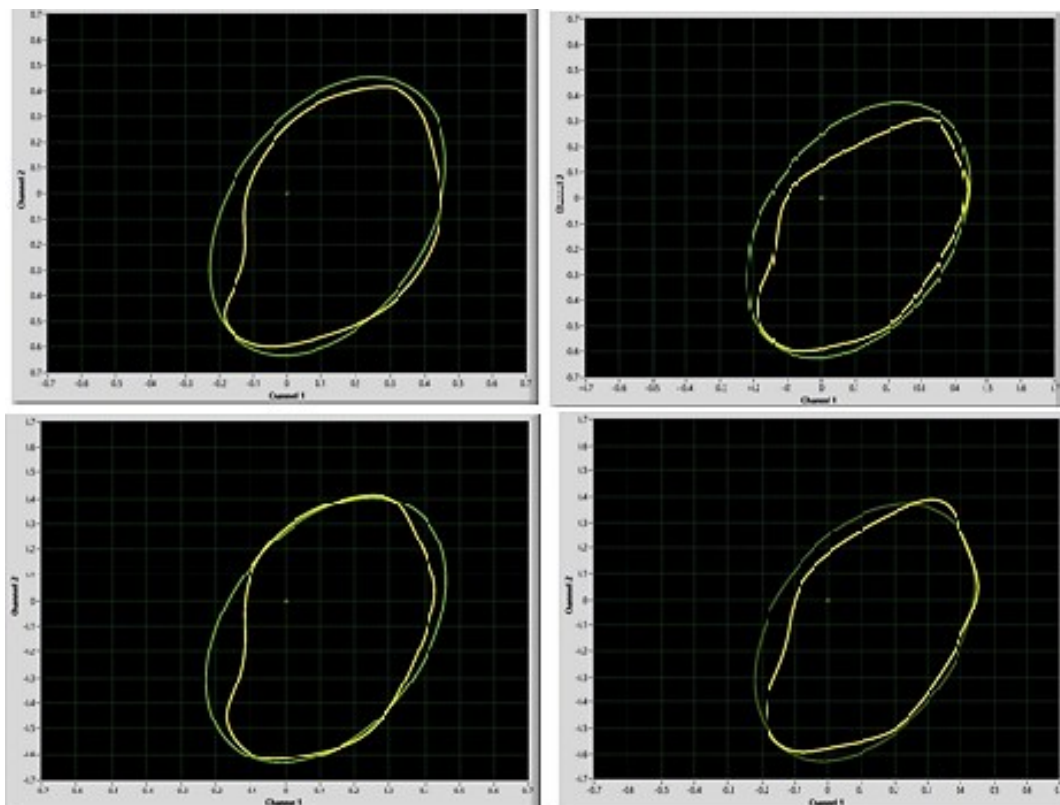


Figure 9. Orbit shapes for shaft journal rotates in SAE 40 oil, for four cases (see text).

## 5. Conclusions

From the discussion and comparison of the experiment and theoretical results, and investigating the main parameter of the rotor system and the surrounding fluid on the dynamic behavior, the following conclusions can be derived:

1. In general the numerical results of the mathematical model is in a good agreements with experiments where the maximum error in calculating the critical speeds is not exceeded 6.8%
2. Using of high viscose fluid such as oil as a surrounding fluid tend to reduce the amplitude of the immersed rotor unbalance response (up to 60%) and resulting better behavior of the rotor system. This is due the damping effect of the interacted fluid.
3. The fluid damping has slight effect on the critical speeds of the rotor, however the size and the location of the attached disc has the predominate effect on the critical speeds.
4. The orbit response of the rotor is affected by the viscosity and damping mechanism of the interacted fluid, it is found that the orbit shape become more irregular as the viscosity of the fluid is increased.

## References

- [1] Jeffcot H. H., "The Lateral Vibration of Loaded Shafts in the Neighborhood of a Whirling Speed: The Effect of Want of Balance," Philosophical Magazine, Series No. 6, Vol. 37. pp. 304, (1919).
- [2] Rao J. S., "History of Rotating Machinery Dynamics", Springer, pp.'312-321', (2011).
- [3] Adams M. "Rotating Machinery Vibration from Analysis to Troubleshooting", New York, Marcel Dekker (2006).
- [4] F. C. Nelson, "Rotor Dynamics without Equations", International Journal of COMADEM, Issue 10, Vol. 3, pp.'2-10', (2007).
- [5] Paidoussis M. P., Fluid-Structure Interactions: Slender Structures and Axial Flow, New York: Academic Press. (1998).
- [6] Friswell M.I., Penny J.E.T., Garvey S.D., "Model Reduction for Structures with Damping and Gyroscopic Effects", International Conference on Noise and Vibration Engineering (ISMA 25), September 13th-15th, pp.'33', (2000).
- [7] G. H. Jang & S. H. Lee, "Free Vibration Analysis Of A Spinning Flexible Disk Spindle System Supported By Ball Bearing And Flexible Shaft Using The Finite Element Method And Substructure Synthesis", J. of Sound And Vibration, V251(1), 59-78 (2002).
- [8] Darlow M., Murphy B. & Sandor G. "Extension Of The Transfer Matrix Method For Rotor-Dynamic Analysis to Include A Direct Representation of Conical Sections And Trunnions", J. of Mechanical Design, ASME, 102; 1223-129(1980).
- [9] Y. H. & Adams, "The Liner Model for Rotor-Dynamics Properties of Journal Bearing and Seal with Combined Radial and Misalignment Motion", Journal of Sound and Vibration, Issue 131, Vol. 3, pp. '367-378', (1989).
- [10] Jei Y.G., Kim Y.J., "Modal Testing Theory of Rotor-Bearing Systems", Journal of Vibration and Acoustics, Vol. 115, pp.'165-176', April, (1993).
- [11] John Vance, Fouad Z., Brain M., "Machinery Vibration and Rotordynamics" New Jersey, Wiley (2010).
- [12] Mahmud, R.I. Effect of Intermediate Bearing on the Dynamical Behaviour of Elastic Rotors (Theoretical and Experimental Investigations), Alnahrain Collage of Eng. Journal, 2014.
- [13] Clarence W. "Vibration and Shock Handbook", CRC Press Taylor & Francis (2005).
- [14] Mohsin J.J, Mahmud R.I.I, Zainab M.H., "Theoretical and Experimental Investigation of the Dynamical Behaviour of Complex Configuration Rotors" Baghdad College of Eng. Journal 2013.

## Nomenclatures

$A$	Shaft cross sectional area, $m^2$	$I_T$	Transverse moment of inertia, $kg.m^2$
$C_{iz}$	$i^{th}$ bearing damping coefficients, in $z$ axis, $N/m$	$K_{zi}$	$i^{th}$ bearing stiffness, in $z$ axis, $N/m$
$C_{iy}$	$i^{th}$ bearing damping coefficients, in $y$ axis, $N/m$	$K_{yi}$	$i^{th}$ stiffness, in $y$ axis, $N/m$
$c$	Bearing clearance, $m$	$L$	Bearing length, $m$
$D$	Bearing diameter, $m$	$L_s$	Shaft span length, $m$
$d_s$	Shaft diameter, $m$	$m_d$	Disc mass, $kg$
$E$	Modulus of elasticity, $N/m^2$	$N$	Mode number or $RPM$
$r$	Disc eccentricity, $m$	$p$ or $p(t)$	Generalized coordinate at $y$ axis
$I$	Area second moment of inertia, $m^4$	$q$ or $q(t)$	Generalized coordinate at $z$ axis

$F_{zs}$	spring forces at z axis, $N$	$\lambda$	Eigen values of free-free beams
$F_{ys}$	spring forces at y axis, $N$	$\delta$	Dirac delta function
$F_{zD}$	damping forces at z axis, $N$	$Z$	Dimensionless lateral coordinate
$F_{zl}$	damping forces at y axis, $N$	$\rho$	Density, $kg/m^3$
$F_{zlb}$	Imbalance forces at z, y axis, $N$	$\mu$	Oil viscosity, Pa-sec
$M_{zG}$	Gyroscopic moments at z, y axis, $N.m$	$\Omega_s$	Disc spin speed, r/s
$M_{zb}$	Inertial moments at z, y axis, $N.m$	$\Omega$	Natural frequency, r/s
$I_p$	Polar moment of inertia, $Kg.m^2$		